Characterization of Polyurethane Foam Reinforced with Seashell Waste Composites: Effects of Filler Type, Loading, and Particle Size

Supachai Kaewjang, and Thanate Ratanawilai *

Seashell waste bio-filler in polymeric material composites sustainably improves insulating performance. This study focuses on polyurethane foam composites (PUFc) reinforced with seashell waste powders and the effects of shell type, particle size, and filler loading on physical and mechanical properties and thermal conduction. Oyster, green mussel, and cockle shells were processed into 20, 40, and 80 mesh sizes and integrated into PUF at 10 to 30 wt% using the closed-mold method. Material characterization results shown by X-ray fluorescence analysis revealed calcium carbonate contents of 91 to 96 wt% in all shells. PUF with 20 wt% fillers, at 40 mesh, increased density, hardness, tensile strength, and compressive strength compared with neat PUF. The optimal formulation, oyster shell density (191 kg/m³), and cockle shell achieved a hardness of 86.7 Shore A. Tensile and compressive strengths were 1580 and 1352 kPa, respectively. Thermal conductivity slightly increased with filler additions. The optimal formulation of 20 wt% at 40 mesh oyster shell was 0.0472 mW/mK. However, water absorption increased with increasing filler content and particle size. Scanning electron microscopy-energy dispersive X-ray microstructural observations indicated improved filler dispersion and preserved closed-cell morphology at 20 wt%, 40-mesh filler loadings, values supporting the suitability of seashell-reinforced PUF as a sustainable building insulation material.

DOI: 10.15376/biores.21.4.11228-11246

Keywords: Polyurethane foam; Seashell waste; Characterization; Insulation

*Contact information: Department of Industrial and Manufacturing Engineering, Faculty of Engineering, Prince of Songkla University, Hat Yai, Songkhla, Thailand; *Corresponding author: thanate.r@psu.ac.th*

INTRODUCTION

Insulation materials have proven to be an effective technology for reducing energy consumption and thus contributing to the sustainability of buildings (Hernando Castro *et al.* 2025). However, roof insulation solutions vary according to the different types of insulation materials used and make unique demands on technology and execution. Roof insulation is considered one of the most effective methods employed in residential and industrial buildings for saving energy and lowering energy costs. As a result, there is less heat loss, less noise transmission, increased energy efficiency, as well as potential fire and moisture resistance. Moreover, each material has its own advantages and disadvantages, which must be carefully chosen according to their physical, mechanical, and thermal properties. Effective thermal insulation materials exhibit low thermal conductivity (typically 0.045 to 0.070 W/(m·K) for bio-based composites), low density (<200 kg/m³), low water absorption (<15%), and compressive strength ranging from several hundred to

several thousand kPa, depending on their composition and structure, thereby ensuring durable thermal performance (Asfaw *et al.* 2024; Luo *et al.* 2026). Effective insulation reduces heat transfer, absorbs sound, improves energy efficiency, and provides fire and moisture protection. However, each material has its benefits and drawbacks, so careful selection is important based on physical, mechanical, and thermal properties (Deraman *et al.* 2022; Dukarska *et al.* 2022).

Polyurethane foam (PUF) is one of the most widely used plastic materials for many different applications. The PUF market continues to grow steadily, with its global value estimated at USD 49.5 billion in 2023 and projected to reach USD 67.8 billion by 2028, reflecting a compound annual growth rate of 6.5% (Wieczorek *et al.* 2025). PUF is considered a sustainable material. In engineering applications beyond insulation, PUF replaces plastics and metals (Barszczewska-Rybarek *et al.* 2022). Insulation material is valued for its great thermal performance, easy application, light weight, and water resistance (Wiyono *et al.* 2016; Fidan and Ertaş 2020). Thereafter, PUF materials exhibit porosity exceeding 95%, primarily due to closed pores. This contributes to low thermal conductivity, high compressive strength, and a wide applicable temperature range (−110 to 200 °C). Additionally, PUF materials have low water absorption, excellent anti-degradation properties, and strong bonding performance (Wang *et al.* 2023). A considerable number of studies have reported that PUF with wood and bamboo fibers and rice husks resulted in increased compressive strength and low thermal conductivity of 0.045 to 0.065 $W.m^{-1}K^{-1}$. The material is regarded as environmentally friendly and lightweight. It has been deemed suitable for application as building bio-based thermal insulation (Shao *et al.* 2020). The PUF reinforced with natural henequen fibers exhibits promising potential as a sustainable material, with compressive yield stress and flexural strength increasing by up to 71% and 40%, respectively (Pech-Can *et al.* 2024). However, PUF exhibits low fire resistance and releases smoke and toxic combustion products during burning, which has driven the development of environmentally friendly PUF composites (Olcay and Kocak 2022).

Seashell waste has become an increasingly important environmental issue associated with the rapid growth of shellfish production worldwide. Every year, the global production of waste oyster, clam, scallop, and mussel shells reaches close to 10 million tons. The disposed shells are frequently dumped at sea or sent to landfills, where they modify soils, waters, and marine ecosystems, thereby creating environmental pollution problems (Suryawanshi *et al.* 2019; Popovic *et al.* 2023). Waste seashells from aquaculture are a major source of biogenic calcium carbonate and can potentially substitute for conventional ground calcium carbonate. Seashells consist primarily of calcium carbonate ($CaCO_3$), accounting for approximately 95% of their composition. Previous studies reported that oyster shell powder improved the maximum elongation of polymer composites. In addition, seashell-derived $CaCO_3$ exhibits high thermal stability and resists decomposition at temperatures between 500 and 700 °C, which may contribute to improved thermal stability and fire resistance of polyurethane foam composites (Basile *et al.* 2024). In Thailand, seashells have been increasingly utilized, and seashell farming and production have increased (Srichanachaichok and Pissuwan 2023). Consequently, there has been an increase in seashell waste. The seafood industry reports producing around 50,000 tons of shell waste annually (Smithmaitriea *et al.* 2020). Over 10 million tons of seashells produced annually worldwide, with oyster, cockle, scallop, and mussel shells accounting for more than 70% of this total, and when shell waste is combined with bioplastics it enables sustainable, eco-friendly materials for applications in the packaging, construction,

and automotive industries (Stopic *et al.* 2023). This shell waste can pollute the area where it is discarded due to the bad smell from the decomposition of residual attached meat and greenhouse gas emissions from the seashells (Zhan *et al.* 2021). These shell wastes can be used as a bioresource and composite biological material linked with multifunctional roles in sustaining ecosystem services. Additionally, shells offer mechanical strength and structural support to PUFc (Chakraborty *et al.* 2020).

Insulation composite materials (ICM) with polyurethane content are increasingly being used as insulators for roofs, floors, ceilings, and walls due to their reasonable cost and excellent heat and sound absorption characteristics (Wang *et al.* 2023). There is also a significant trend to improve the overall properties of such mechanical and thermal improvements manufactured from polyurethane. Manufacturing foam-type polyurethane engineered composites reinforced with various types of additives is one of the approaches to enhance not only their mechanical properties but also other characteristics, including thermal insulation quality (Akdogan and Soykan 2025). Using waste material from seashells as a reinforcement agent to produce polyurethane foam composite (PUFc) would be considered an alternative way to improve the overall properties of such engineered panel products. The incorporation of tidal seashell powder into epoxy composites increased density (2%) and improved tensile strength in the range of 10 to 17 MPa; however, excessive filler content reduced mechanical performance due to agglomeration effects (Kıstak *et al.* 2025). It is obvious that productively value-added composites reinforced with underutilized material will be environmentally friendly and reduce the adverse impact of waste in the form of landfills and pollution. Currently, limited information is available regarding the comparative effects of different seashell species on the physical, mechanical, and thermal performance of polyurethane foam composites. Furthermore, limited information exists on the mechanical performance of polymer-based panel systems. In this study, oyster, cockle, and green mussel shells were selected as reinforcing fillers for PUFc. According to the Department of Fisheries, Thailand, these three species represent the major cultivated marine shellfish in Thailand, accounting for 49.43%, 36.04%, and 14.53% of total production in 2024, respectively. Therefore, they constitute the most abundant and readily available sources of seashell waste. The working hypothesis is that differences in shell type, composition, and particle size distribution among oyster, cockle, and green mussel shells may lead to varying reinforcing efficiencies in PUF systems. Accordingly, the objective of this study was to develop polyurethane foam composites reinforced with oyster, cockle, and green mussel shell powders and to evaluate their physical, mechanical, and thermal properties for building insulation applications. These PUFc reinforced with $CaCO_3$ derived from seashell waste may be suitable for rigid roof insulation and prefabricated building components such as wall panels and cold storage systems. Because of their low density and moisture resistance, these materials are expected to perform reliably under humid and elevated temperature conditions. The addition of $CaCO_3$ also is expected to improve mechanical integrity, enabling the composites to withstand structural loading. Compared with conventional insulation materials, the composites exhibit comparable thermal performance without an increase in density. Improved mechanical properties extend their applicability to load-bearing structural applications, whereas the incorporation of seashell-derived fillers facilitates waste valorization and reduces dependence on chemical additives, thereby enhancing their potential for energy-efficient construction.

EXPERIMENTAL

Materials

PUF, a commercial rigid polyurethane made from polyol (agent A) and isocyanate (agent B), was supplied by Dow Chemical Thailand, namely VORACOR™ CM938 polyol and PAPI™ 27/135C polymeric MDI. The polyol component had a hydroxyl number of 270 to 310 mg KOH/g, a viscosity of 700 to 1000 mPa·s, and a specific gravity of 1.02 g/cm³. The polymeric MDI (pMDI) exhibited an NCO content of 31.0%, a viscosity of 210 mPa·s, and a specific gravity of 1.23 g/cm³. The two components were mixed at a weight ratio of 1:1 to preparation. Three seashell wastes for reinforcement were oyster "*Crassostrea gigas*," mussel "*Perna viridis*," and cockle "*Anadara granosa*" collected from the coastal area of the Gulf of Thailand. Thereafter, seashells were thoroughly cleaned and then sun-dried for two days before being oven-dried at 100 °C for 1 h. Subsequently, seashells were ground to a fine powder using a ball mill at 350 rpm for 5 to 10 min. Seashell powder was sieved into three particle size ranges: 20 mesh (0.841 mm), 40 mesh (0.400 mm), and 80 mesh (0.149 mm), as shown in Fig. 1.

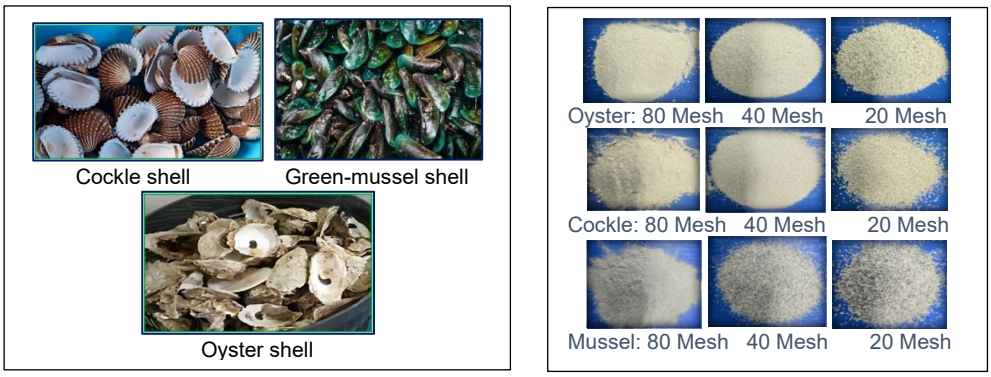


Fig. 1. Type and particle size of seashells

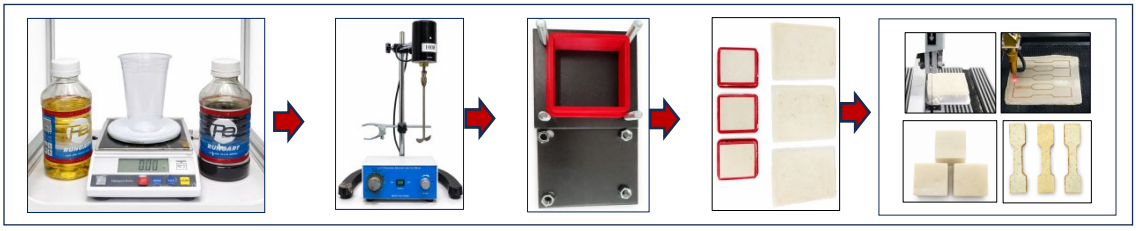


Fig. 2. Sample processing preparation

Methods

Preparation of sample

The manufacturing process for preparing PUFc material insulation (Li *et al.* 2019) is close-mold compressive, with the mold designed and created by the 3D printing process. Initially, polyol was mixed with seashell waste, stirring at 1200 rpm for 60 s. The mixture was then subjected to the addition of isocyanate, which was stirred at 1200 rpm for 30 s to initiate the polymerization. Based on the application, the reactive liquid was poured into a mold. Afterwards, the PUF composite material was cured at room temperature for 1 h to allow the solid stage. Finally, PUFc was sawn to the desired dimension before testing the specimens, shown in Fig. 2.

Experimental design

The experimental design used a full factorial design because there were 3 factors and 3 levels (seashells: oyster, mussel, and cockle; ratio: 10, 20, and 30 wt%; and particle size: 20, 40, and 80 mesh) being studied. The composites were coded as PU/OYx–yM, where *x* denotes filler loading (wt%) and *y* indicates particle size (mesh), which are 28 constraints shown in Table 1. These PUF composites were evaluated for chemical structure (X-ray Fluorescence (XRF)), density, hardness, tensile strength, compressive strength, thermal conductivity, and water absorption. The microstructure was investigated using Scanning Electron Microscopy (SEM). The optimal formulation was determined based on a performance assessment of PUFc.

Table 1. The Formulation Proportions Code of the PUFc

No	PUFc Code	No	PUFc Code	No	PUFc Code	No	PUFc Code
1	PU100	*8*	PU/Oy10-20M	*15*	PU/Mu20-40M	*22*	PU/Co30-80M
2	PU/Oy10-80M	*9*	PU/Oy20-20M	*16*	PU/Mu30-40M	*23*	PU/Co10-40M
3	PU/Oy20-80M	*10*	PU/Oy30-20M	*17*	PU/Mu10-20M	*24*	PU/Co20-40M
4	PU/Oy30-80M	*11*	PU/Mu10-80M	*18*	PU/Mu20-20M	*25*	PU/Co30-40M
5	PU/Oy10-40M	*12*	PU/Mu20-80M	*19*	PU/Mu30-20M	*26*	PU/Co10-20M
6	PU/Oy20-40M	*13*	PU/Mu30-80M	*20*	PU/Co10-80M	*27*	PU/Co20-20M
7	PU/Oy30-40M	*14*	PU/Mu10-40M	*21*	PU/Co20-80M	*28*	PU/Co30-20M

Characterization of PUFc

The characteristic testing methodologies of PUFc insulation materials were according to ASTM standards. The evaluation process involved assessing the mechanical, physical, and thermal conductivity properties of specimens under representative conditions. This process ensured the reproducibility and validity of the results, reinforcing the composite material's suitability for industrial insulation.

X-ray Fluorescence (XRF): The Zetium XRF spectrometer and XRF analysis of seashells were used to determine the elemental composition and calcium carbonate ($CaCO_3$) content, which are both components of seashells.

Density: Following ASTM D3574 (2017) Test A, the specimens of regular squares were 50 mm × 50 mm × 25 mm, with three specimens tested each. The density was calculated in kilograms per cubic meter.

Hardness: Following ASTM D2240 (2015) Shore A durometer, the specimens were 50 mm × 50 mm × 25 mm, with three specimens tested per sample.

Tensile strength: Following ASTM D3574 (2017) Test E, the dumbbell specimens' thickness was 6 mm at a speed of 3 mm/min, testing three specimens per sample.

Compressive strength: Following ASTM D1621 (2023), the test specimens were 50 mm × 50 mm × 25 mm, testing three specimens per sample. The compression was obtained from the stress-strain curve at a deformation of 10%.

Thermal conductivity: The thermal conductivity was measured using a FOX 200 heat flow meter (TA Instruments) in accordance with ASTM C518 (2017). The specimens had dimensions of 100 mm × 100 mm × 50 mm, and three specimens were tested for each sample.

Water absorption: In accordance with ASTM D570-98 (2018), specimens measuring 50 mm × 50 mm × 25 mm were utilized, with three specimens tested each sample.

Scanning electron microscopy-energy dispersive X-ray (SEM-EDX): An FEI Quanta SEM was used for elemental mapping with an EDX detector, model XMAX 03.

Statistical analysis

Statistical analyses were performed using the statistical software (Minitab, LLC, version 22.4, State College, PA, USA). All experiments were conducted in triplicate, and the results are presented as mean ± standard deviation. Differences among groups were evaluated using one-way analysis of variance (ANOVA), followed by Tukey's honestly significant difference (HSD) test at a significance level of $p < 0.05$.

RESULTS AND DISCUSSION

XRF Analysis

The XRF results and calculated calcium carbonate ($CaCO_3$) content were estimated from XRF analysis in seashell waste to determine their compositions, with calcium reported as calcium oxide (CaO). Seashell waste material was the assumption of $CaCO_3$. Consequently, CaO contents from XRF analysis were converted to $CaCO_3$ using stoichiometric molar mass relationships. The conversion from CaO to $CaCO_3$ was based on the molar masses of CaO (56.077 $g \cdot mol^{-1}$) and $CaCO_3$ (100.086 $g \cdot mol^{-1}$), resulting in a conversion factor of 1.7848. The $CaCO_3$ content was calculated using Eq. 1. The results of the $CaCO_3$ content in seashell waste are summarized in Table 2. The analyzed seashell wastes exhibited high $CaCO_3$ contents ranging from 91 to 96 wt%, with cockle shell showing the highest proportion. In addition to $CaCO_3$, minor amounts of Na_2O, MgO, Al_2O_3, SiO_2, P_2O_5, SO_3, K_2O, Fe_2O_3, and SrO were detected by XRF. These constituents accounted for approximately 4 to 9 wt.% of the shell composition. Such elevated $CaCO_3$ levels confirm the mineral-rich nature of the biogenic materials and indicate their potential suitability as sustainable bio-fillers in composite applications. Comparable $CaCO_3$ contents in seashell waste have been reported in recent studies employing XRF-based stoichiometric conversion methods (Ahad *et al.* 2023), demonstrating strong agreement with previously published findings. $CaCO_3$ content was calculated as follows:

$$CaCO_3\ (\%) = CaO\ (\%) \times 1.7848 \quad (1)$$

Table 2. CaO Concentrations and Calculated $CaCO_3$ Contents of Seashells Waste

Seashells	CaO (wt%)	$CaCO_3$ (wt%)
Oyster	52.49	93.69
Cockle	53.71	95.84
Green Mussel	51.22	91.41

Density of the Samples

The density testing results, as shown in Fig. 3 indicated that for PU100 (95.07 kg/m^3), the incorporation of seashell-derived $CaCO_3$ at 10 to 20 wt% increased the composite density, with measured values ranging from 69 to 192 kg/m^3. The highest densities were obtained at 20 wt% filler content with 40 mesh. Under this condition, the

oyster shell composite reached 191 kg/m³, followed by green mussel (186 kg/m³) and cockle shell (174 kg/m³). The increase in density at 20 wt% is attributed to improved solid content within the polymer matrix and restriction of foam expansion during cell formation. At this loading level, particle dispersion was sufficient to enhance structural compactness without severely disrupting cell growth. However, when the filler loading was increased to 30 wt%, the density decreased. This reduction is associated with particle agglomeration and non-uniform cell development, which can introduce voids within the foam structure. Density is also influenced by particle size. Composites prepared with 20 mesh showed lower densities, which is likely due to less uniform dispersion in the reactive mixture. In contrast, 40 and 80 mesh produced higher densities than neat PU, indicating greater restrictions on expansion during foaming.

Similar trends have been reported for $CaCO_3$-filled polyurethane systems, where moderate filler contents improve structural compactness, whereas excessive loading promotes agglomeration and morphological irregularity (Ahad *et al.* 2023; Kıstak *et al.* 2025). Particle-size effects on interfacial contact and dispersion efficiency have likewise been observed in waste-derived filler composites (Kuciel *et al.* 2024).

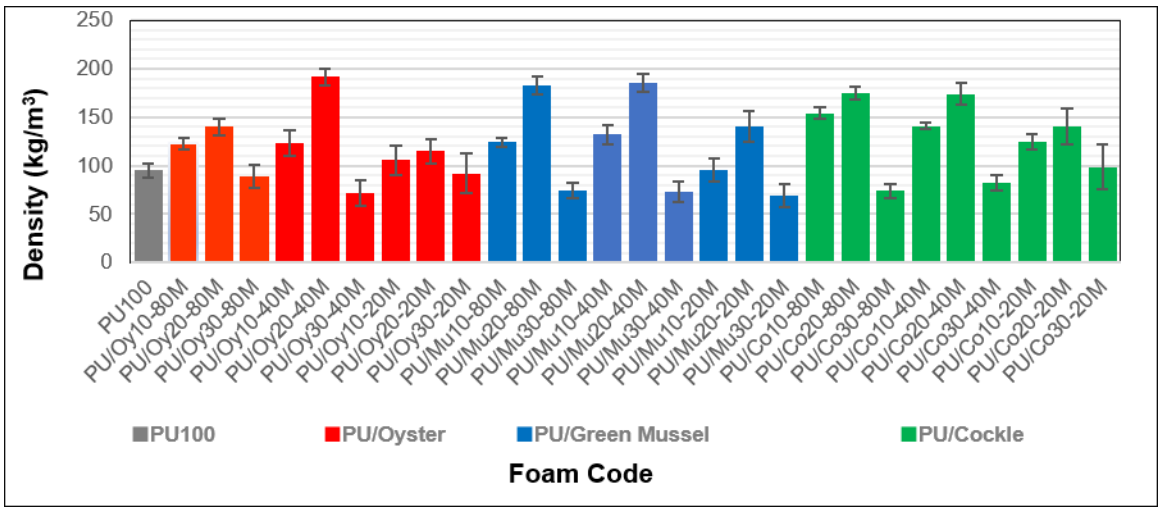


Fig. 3. Density of PUFc

Hardness of the Samples

The hardness result, as shown in Fig. 4, indicated that PU100 exhibited a Shore C hardness of 70.53 and served as the reference biomaterial. Incorporating seashell waste fillers in proportions of 10 wt% and 20 wt% increased hardness compared with PU100. The hardness of the PUF composites ranged from approximately 75.7 to 83.8 at 10 wt% and 77.3 to 86.7 at 20 wt%, with cockle shells exhibiting the highest hardness, followed by those containing green mussel shell-reinforced filler and oyster shell-based filler. In contrast, increasing the seashell filler content to 30 wt% reduced the hardness, with values ranging from 56.2 to 71.0. Particle sizes of 80 mesh and 40 mesh increased in hardness, ranging from 67.0 to 86.9 at 80 mesh, 69.9 to 86.7 at 40 mesh, and 66.4 to 82.3 at 20 mesh. Hardness tended to increase when seashell particle sizes of 80 and 40 mesh were incorporated as filler infill from 10 wt% to 20 wt%, indicating effective reinforcement and improved hardness within the polyurethane matrix. In contrast, the use of a coarse particle size of 20 mesh at a high filler infill of 30 wt% resulted in a noticeable reduction in hardness. This decrease is likely associated with poor particle dispersion and disruption of

the foam structure at excessive filler content, which adversely affected the mechanical integrity of PUF composites. The hardness results indicated that all types and proportions of seashells with 20 wt% filler content and 40 mesh showed high hardness values. Adding bio-seashells enhanced the surface resistance properties, which is desirable for ICM.

The hardness values obtained in this study (75.7 to 86.7 Shore C) were within the range reported for $CaCO_3$-filled polyurethane composites in previous studies. Similar improvements in hardness at moderate $CaCO_3$ loadings have been reported in polyurethane systems, where enhanced rigidity and improved stress transfer occur at 10 to 20 wt% filler content, while excessive loading (> 30 wt%) leads to agglomeration and reduced mechanical performance (Ahad *et al.* 2023). Particle size effects have also been documented, with finer $CaCO_3$ fractions promoting better dispersion and interfacial interaction compared with coarse particles (Kuciel *et al.* 2024).

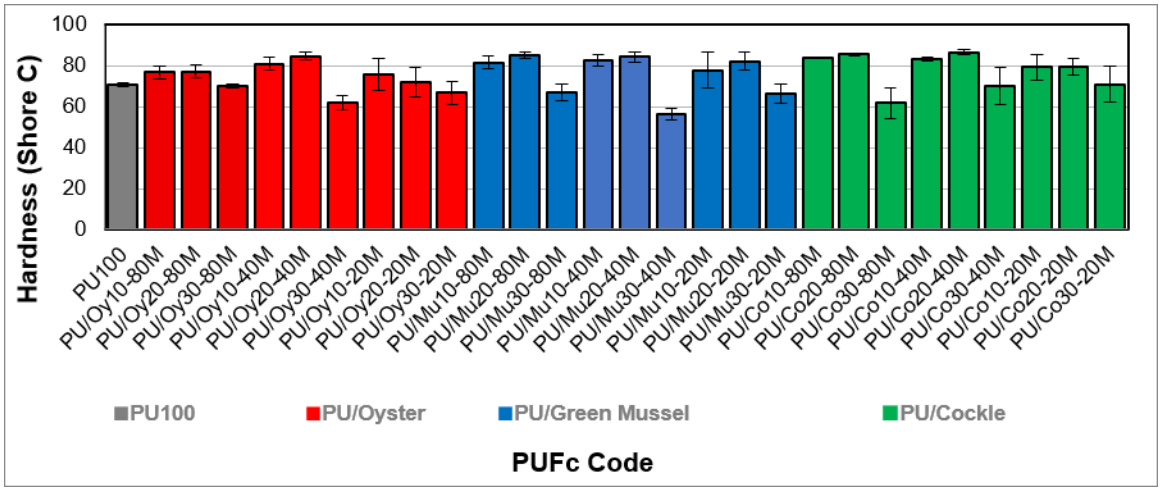


Fig. 4. Hardness of PUFc

Tensile Strength of the Samples

Results of tensile tests of the samples are displayed in Figs. 5 and 6. The PU100 was 727 kPa (60 N). The addition of seashell fillers improved tensile strength, with cockle shell composites showing the highest values, followed by oyster shell and green mussel. Green mussel composites exhibited lower strength, particularly at larger particle sizes and higher filler contents. Particle size had a strong effect, as 40 mesh consistently provided higher tensile strength than 80 or 20 mesh. The 20 mesh filler is expected to have reduced performance due to stress concentration and weaker interfacial bonding. Increasing filler content from 10 to 20 wt% enhanced tensile strength, whereas 30 wt% caused a considerable decrease, which is attributed to particle agglomeration and cell structure disruption. The highest tensile strength (1580 kPa) was obtained for PU/Co20–40M (130 N), more than twice that of PU100, while 30 wt% at 20 mesh showed the lowest values. Optimal tensile performance was achieved with cockle shells at 40 mesh and 20 wt% loading.

The tensile strength enhancement observed at moderate filler contents (10 to 20 wt%) is consistent with previous studies on $CaCO_3$-modified polyurethane foams. For example, Kustiyah *et al.* (2022) reported that PUF coated with low fractions of $CaCO_3$ exhibited improved tensile strength and changes in cell morphology attributable to the incorporation of the mineral phase. The effect of $CaCO_3$ on reinforcing foam structure suggests that filler distribution and interaction with the matrix are critical factors

influencing mechanical performance. Moreover, other reports indicate that varying $CaCO_3$ contents can modify mechanical properties in PUF systems, implying that optimal filler loading is necessary to balance reinforcement without inducing structural disruption at higher contents (Ebereonwu *et al.* 2022).

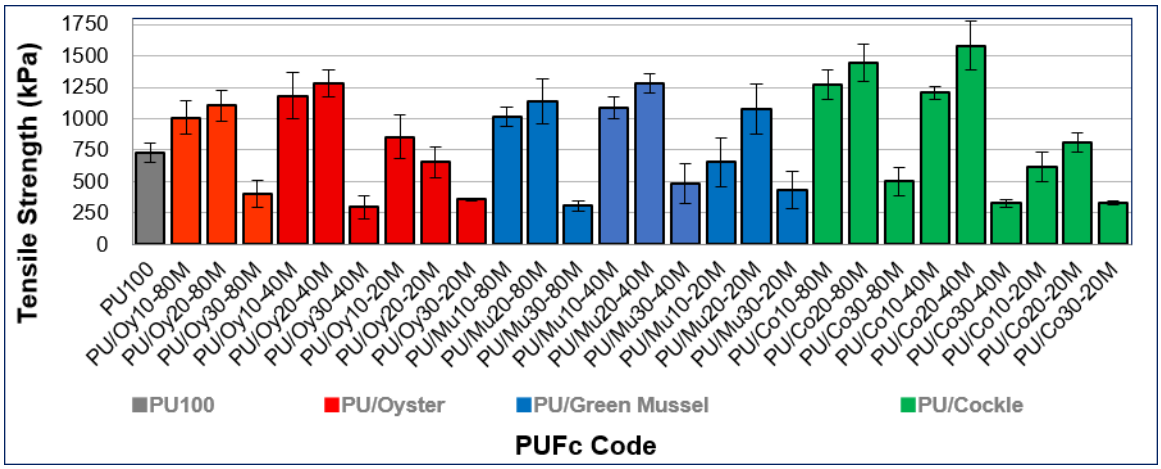


Fig. 5. Tensile strength of PUFc

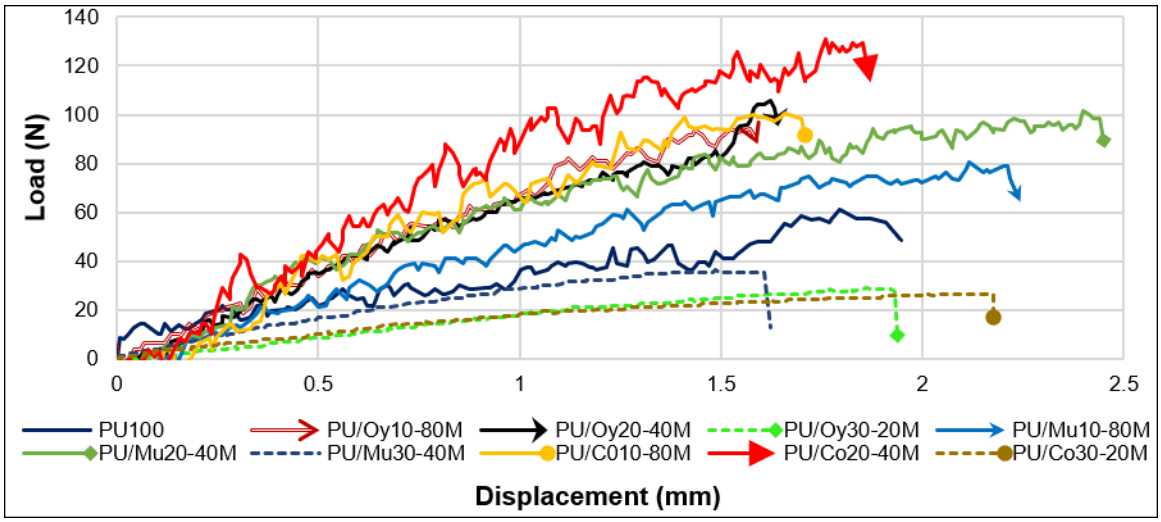


Fig. 6. Load *vs* Displacement of PUFc

Compressive Strength of the Samples

The compressive strength of PU100 was 299 kPa (675 N), as shown in Figs. 7 and 8. The addition of seashell fillers improved compressive strength. Cockle shell composites exhibited the highest values, followed by oyster shell and green mussel shell. In particular, cockle shell provided superior load-bearing capacity and stress transfer under compression, while green mussel composites showed lower performance, especially at larger particle sizes and higher filler contents. Particle size had a strong influence, as 40 mesh consistently produced higher compressive strength than 80 and 20 mesh. This suggests improved dispersion and reinforcement at 40 mesh, whereas 20 mesh reduced strength due to non-uniform stress distribution and premature foam cell collapse. Increasing filler content from 10 wt% to 20 wt% enhanced compressive strength, but 30 wt% led to a sharp decline,

which was attributed to cell structure disruption and particle agglomeration. The highest compressive strength (1350 kPa) was obtained for PU/Co20–40M (3467 N), more than four times that of PU100. In contrast, composites with 30 wt% at 20 mesh showed the lowest values. Optimal compressive performance was achieved using cockle shells at 40 mesh with 20 wt% loading, promoting structural stability and efficient stress distribution.

The increase in compressive strength with up to 20 wt% seashell content is consistent with reports on $CaCO_3$-filled PUF, where adding filler improved compressive performance by reinforcing the cellular structure and enabling more effective stress transfer between particles and the polymer matrix (Choe *et al.* 2020). Similar trends have been observed with moderate additions of inorganic or fiber-based fillers, which enhanced compressive strength and modulus relative to unmodified PUF, provided that adequate dispersion and cell integrity were maintained (Bello and Yan 2024).

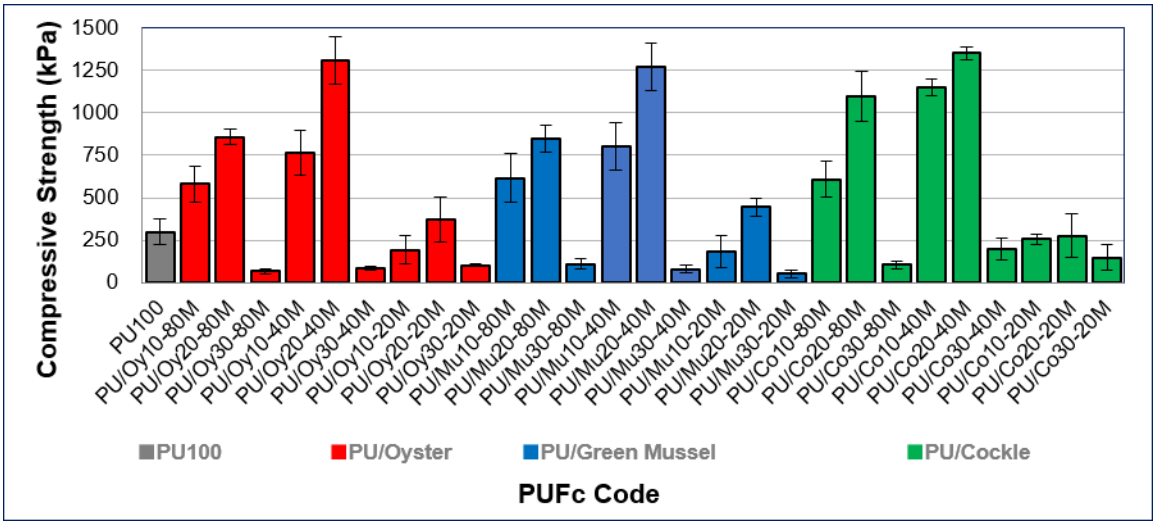


Fig. 7. Compressive strength of PUFc

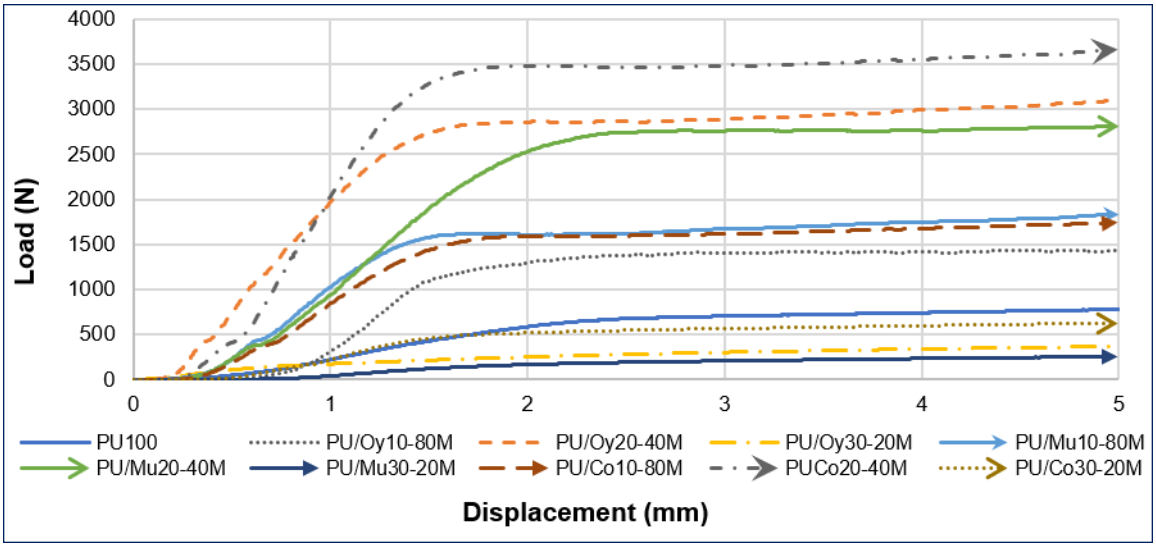


Fig. 8. Load *vs* Displacement of PUFc

Water Absorption of the Samples

Water absorption of PU100 was low (2.09 wt%), as shown in Fig. 9. The incorporation of seashell fillers increased water uptake, depending on filler characteristics and loading level. Among the seashell types, oyster shell composites showed the lowest water absorption, followed by cockle shell and green mussel, while green mussel exhibited the highest values, particularly at higher loadings. Particle size had a clear effect. Composites with 20 mesh showed higher water absorption than those with 40 and 80 mesh due to interfacial voids and microgaps that facilitated water penetration. In contrast, 80 mesh resulted in lower water uptake, indicating improved dispersion and reduced porosity. Water absorption increased with increasing filler content. Composites with 10 and 20 wt% filler exhibited relatively low values, while 30 wt% considerably increased water uptake. The highest value (35.7 wt%) was observed for PU/Mu30–20M. Overall, moisture resistance was lowest using oyster shell, fine particles (80 mesh), and low filler content (10 wt%).

Similar behavior has been reported in bio-filled polyurethane foams. Anwar *et al.* (2023) found that filler incorporation modified cell morphology and increased water uptake compared with neat foams, emphasizing the role of filler distribution and foam structure in moisture absorption. These findings support the present results that water uptake in PUF composites is governed by both filler characteristics and cellular structure.

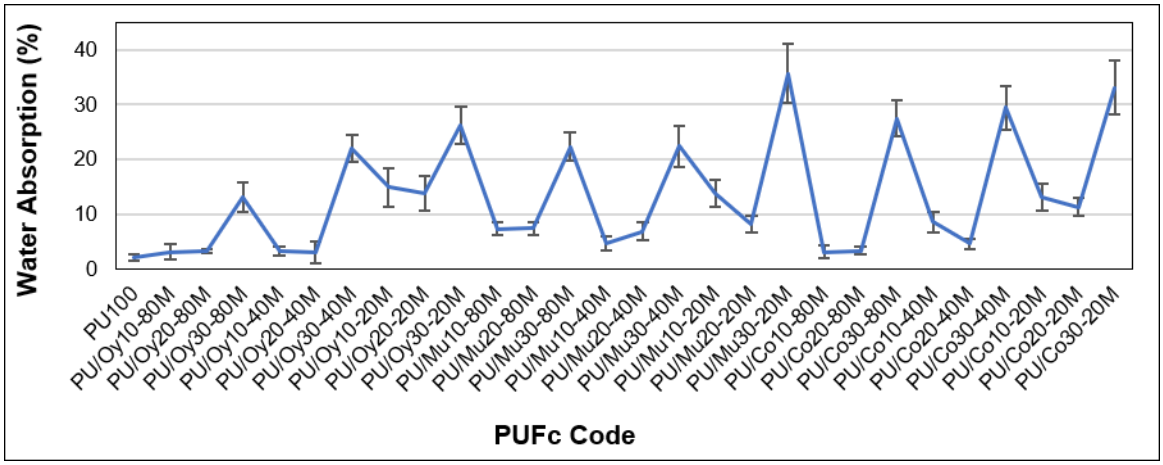


Fig. 9. Water absorption of PUFc

Thermal Conductivity of the Samples

As shown in Fig. 10, oyster shell thermal conductivity yielded the lowest values among the fillers, followed by cockle and green mussel shells. PU100's thermal conductivity was 45.1 mW/mK, but the others were not considerably different. The addition of seashell powder slightly increased thermal conductivity. Composites with 20 mesh showed higher thermal conductivity than those with 40 and 80 mesh, while 80 mesh generally maintained lower values. Increasing filler content from 10 to 30 wt% caused a gradual rise in thermal conductivity due to additional heat transfer pathways. The highest value (57.8 mW/mK) was obtained for PU/Gr30–20M, whereas the lowest (48.0 mW/mK) was observed for PU/Oy10–80M. Filler contents of 10 to 20 wt% combined with small to medium particle sizes, particularly oyster shell, were more effective in maintaining insulation performance, yielding thermal conductivity values close to those of PU100 and making this formulation optimal for insulation applications.

Several recent studies on rigid PUF with inorganic fillers have reported similar thermal conductivity behavior, where the addition of mineral particles caused modest increases in thermal conductivity values, particularly at higher filler contents. The thermal conductivity showed an increasing trend with increasing filler content. This behavior is often linked to the formation of continuous solid conduction paths within the foam and changes in cellular architecture that facilitate heat transfer through the matrix. Similar observations have been reported for PUF reinforced with microspheres (Hadała *et al.* 2024). Additionally, reviews of thermal properties in PUF systems show that both filler characteristics and cell morphology affect heat-transfer performance, with finer and more uniformly distributed particles limiting conductivity increases compared with coarse or poorly dispersed fillers (Fadhil *et al.* 2024).

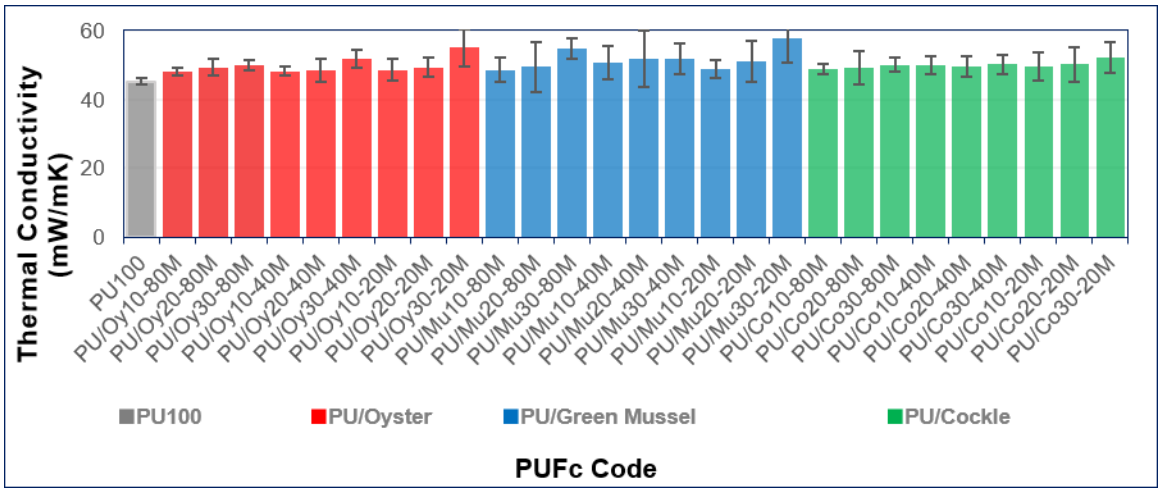


Fig. 10. Thermal conductivity of PUFc

SEM–EDX of the Samples

The microstructure and elemental distribution of PUFc reinforced with seashell powders were examined by SEM and EDX (Figs. 11 and 12). PU100 exhibited a uniform closed-cell structure with smooth and regular cell walls. The addition of seashell fillers altered the foam morphology depending on shell type, particle size, and filler content. The comparatively uniform cellular structure of the PUF matrix was indicative of its exceptional compatibility with oyster shell composites, particularly at low filler loading and fine particle size. In contrast, composites composed of green mussel and cockle shells exhibited increased cell wall irregularity and deformation, which was further exacerbated by the addition of higher filler concentrations. The particle size exerted a considerable influence. Composites with 80 mesh retained more uniform cells, while 40 mesh showed moderate distortion. Samples including 20 mesh particles had abnormal cells and partial wall breakage resulting from agglomeration and disruption of cell development. Augmenting filler material from 10 to 30 wt% progressively compromised the cellular architecture. At 10 wt%, the dispersion was comparatively uniform. At 30 wt%, cell coalescence and wall failure were apparent, especially with 20 mesh. The matrix contained Ca, C, and O, as confirmed by EDX. Localized Ca-rich regions were observed at 30 wt% and 20 mesh, suggesting agglomeration, while uniform Ca distribution was observed at low to moderate filler contents with finer particles. These regions corresponded to structural discontinuities in SEM. Overall, foam shape was maintained, and dispersion was

enhanced by a low to moderate filler concentration (10 to 20 wt%) with a finer 80 mesh. The structural disruption resulted from oyster shell, whereas cockle shell demonstrated a more considerable morphological alteration with high loading compared to the other additives.

The impact of $CaCO_3$ filler on the microstructure and mechanical properties of PUF composites aligns with recent research findings. Kustiyah *et al.* (2022) showed that chitosan-coated $CaCO_3$ changed the pore architecture and improved tensile strength and thermal stability in PUF. SEM images showed denser cell packing at optimal filler concentrations, indicating that surface-treated $CaCO_3$ fillers changed foam morphology and compressive properties in rigid PUFc, emphasizing how filler surface features affect cellular structure and load distribution.

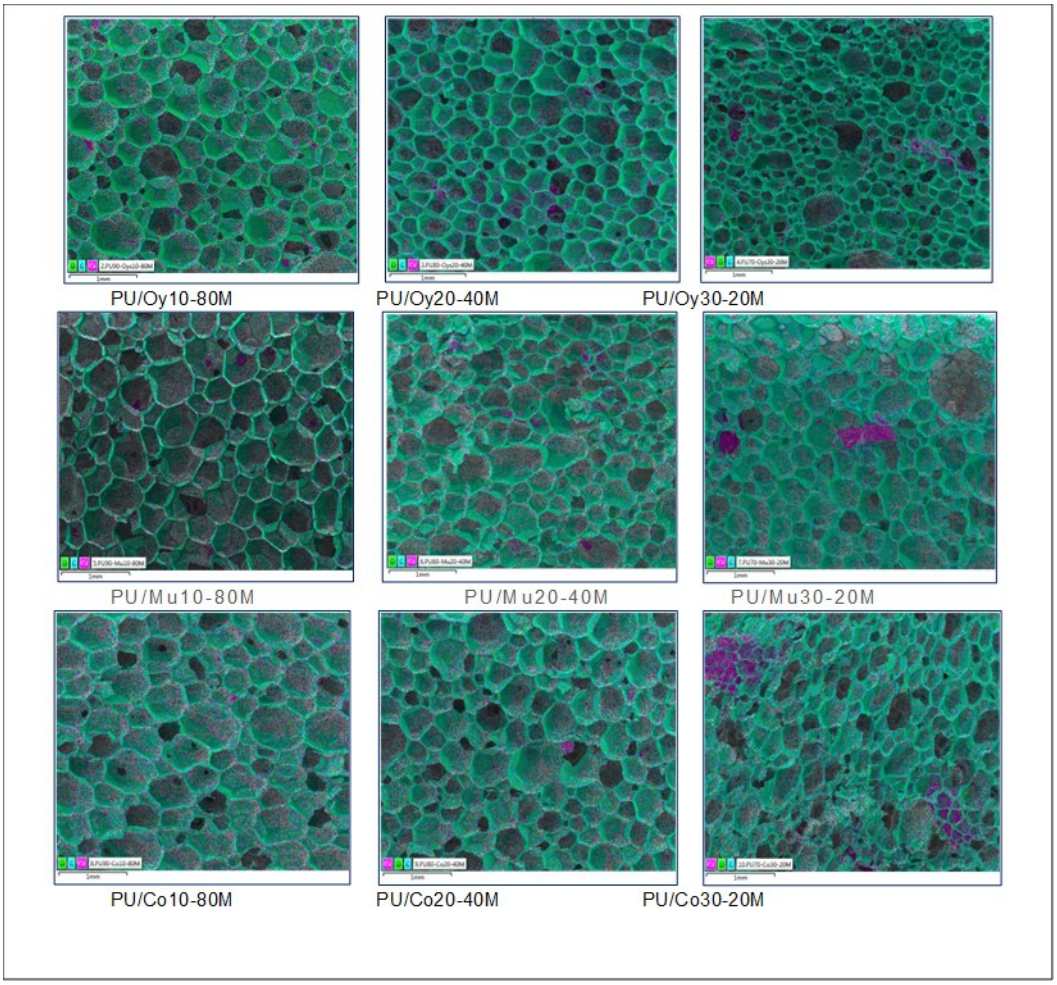


Fig. 11. The EDX images of the PUFc (Magnification: x50, Accelerating voltage: 15 kv)

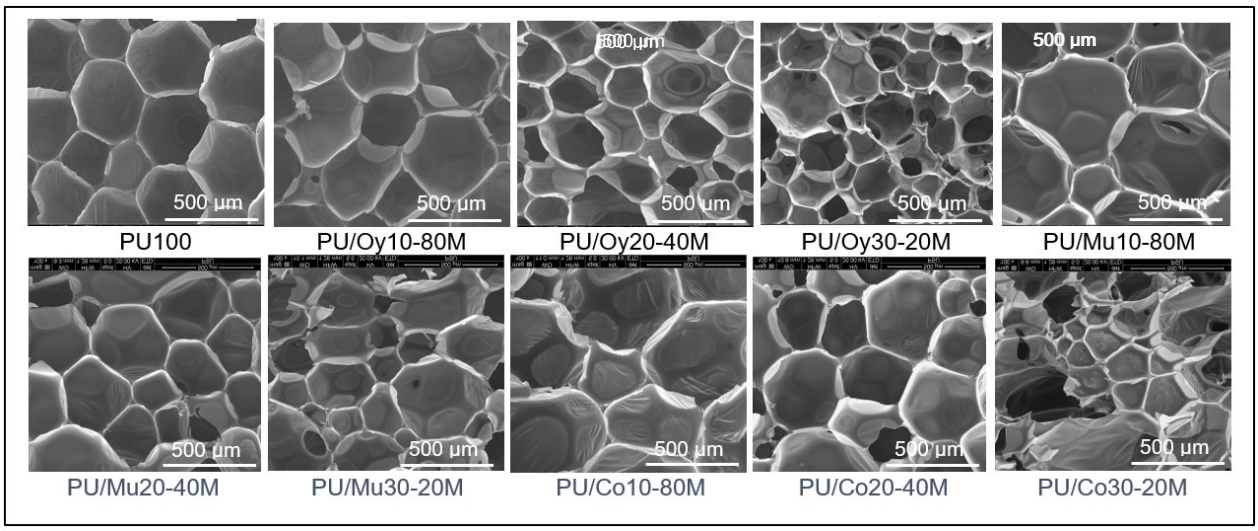


Fig. 12. The SEM images of the PUFc (Magnification: x100, Accelerating voltage: 15 kv)

Table 3. Mean Values and Groups Resulting from the Tukey Analysis of PUFc

PUFc Code	Density (kg/m^3)	Hardness (Shore A)	Tensile Strength (kPa)	Compressive Strength (kPa)	Water Absorption (%)
PU100	95.07$^{E F G H}$	70.53$^{B C D E F G}$	727$^{E F G H I}$	299$^{E F G H}$	2.09^{H}
PU/Oy10-80M	122.91$^{C D E F}$	76.73$^{A B C D E F}$	1010$^{C D E F}$	581$^{C D E}$	3.09$^{G H}$
PU/Oy20-80M	140.41$^{B C D}$	77.27$^{A B C D E}$	1103$^{B C D E}$	857$^{B C}$	3.35$^{G H}$
PU/Oy30-80M	88.67$^{F G H}$	70.07$^{C D E F G}$	400$^{I J}$	67^{H}	13.16^{F}
PU/Oy10-40M	123.25$^{C D E F}$	80.93$^{A B C D E}$	1183$^{A B C D}$	762^{C}	3.27$^{G H}$
PU/Oy20-40M	191.49^{A}	84.67$^{A B C}$	1280$^{A B C}$	1305^{A}	3.11$^{G H}$
PU/Oy30-40M	71.68^{H}	61.67$^{F G}$	297^{J}	83^{H}	22.04$^{C D E}$
PU/Oy10-20M	105.99$^{D E F G H}$	75.73$^{A B C D E F}$	857$^{D E F G}$	193$^{F G H}$	14.86$^{D E F}$
PU/Oy20-20M	114.77$^{D E F G}$	72.07$^{A B C D E F}$	657$^{F G H I J}$	370$^{D E F G}$	13.84$^{E F}$
PU/Oy30-20M	91.80$^{F G H}$	66.80$^{D E F G}$	360$^{I J}$	103$^{G H}$	26.24$^{B C}$
PU/Mu10-80M	123.94$^{C D E F}$	81.67$^{A B C D}$	1013$^{C D E F}$	616$^{C D}$	7.36$^{F G H}$
PU/Mu20-80M	183.06^{A}	85.40$^{A B}$	1137$^{B C D}$	848$^{B C}$	7.45$^{F G H}$
PU/Mu30-80M	74.24^{H}	67.00$^{D E F G}$	307^{J}	111$^{G H}$	22.30$^{C D}$
PU/Mu10-40M	132.37$^{C D E}$	82.80$^{A B C}$	1087$^{B C D E}$	802^{C}	4.74$^{G H}$
PU/Mu20-40M	185.68^{A}	84.20$^{A B C}$	1280$^{A B C}$	1268^{A}	6.81$^{F G H}$
PU/Mu30-40M	73.11^{H}	56.20^{G}	483$^{G H I J}$	81^{H}	22.37$^{C D}$
PU/Mu10-20M	95.22$^{E F G H}$	77.87$^{A B C D E}$	653$^{F G H I J}$	185$^{F G H}$	13.84$^{E F}$
PU/Mu20-20M	140.47$^{B C D}$	82.27$^{A B C}$	1077$^{B C D E}$	445$^{D E F}$	8.18$^{F G H}$
PU/Mu30-20M	69.26^{H}	66.40$^{E F G}$	433$^{H I J}$	52^{H}	35.68^{A}
PU/Co10-80M	154.30$^{A B C}$	83.80$^{A B C}$	1273$^{A B C}$	608$^{C D}$	3.07$^{G H}$
PU/Co20-80M	174.45$^{A B}$	85.47$^{A B}$	1443$^{A B}$	1094$^{A B}$	3.37$^{G H}$
PU/Co30-80M	74.13^{H}	61.73$^{E F G}$	503$^{G H I J}$	105$^{G H}$	27.49$^{A B C}$
PU/Co10-40M	140.73$^{B C D}$	83.40$^{A B C}$	1207$^{A B C D}$	1150^{A}	8.56$^{F G H}$
PU/Co20-40M	173.67$^{A B}$	86.67^{A}	1580^{A}	1352^{A}	4.60$^{G H}$
PU/Co30-40M	82.13$^{A B}$	69.87$^{C D E F G}$	327^{J}	198$^{F G H}$	29.50$^{A B C}$
PU/Co10-20M	124.68$^{C D E F}$	79.27$^{A B C D E}$	617$^{F G H I J}$	255$^{F G H}$	13.09^{F}
PU/Co20-20M	141.00$^{B C D}$	79.47$^{A B C D E}$	810$^{D E F G H}$	277$^{F G H}$	11.28$^{F G}$
PU/Co30-20M	98.70$^{E F G H}$	71.00$^{B C D E F G}$	333$^{I J}$	148$^{G H}$	33.15$^{A B}$

* Means with the same letters are not significantly different (Tukey HSD, $p < 0.05$), n = 3)

Statistical Analysis

Mean values and Tukey groupings showed significant effects ($p < 0.05$) (Saadaoui *et al.*, 2017; Fidan and Ertaş 2020) for the mechanical property of PUFc reinforced with bio-$CaCO_3$ fillers from oyster, green mussel, and cockle shells, as shown in Table 3. The results indicate that filler concentration and particle size greatly affected PU mechanical performance and moisture behavior. Addition of $CaCO_3$ increased mechanical characteristics by enhancing stress transmission between the polymer matrix and foam cell walls (Choe *et al.*, 2020). Furthermore, $CaCO_3$ acted as a nucleating agent during foaming, encouraging a homogeneous cellular structure and increased mechanical strength (Fidan and Ertaş 2020). The formulation with the highest tensile and compressive strengths was observed at 20 wt% filler loading and a particle size of 40 mesh. However, increasing the filler concentration to 30 wt% decreased mechanical characteristics due to particle agglomeration and foam structure rupture. Similarly, water absorption increased with higher filler loading, which was likely due to increased porosity and microstructural defects in the PU matrix. Previous studies also reported that excessive filler loading negatively affects the mechanical performance of PU (Dukarska *et al.* 2022; Bello and Yan 2024). Thus, shell-derived $CaCO_3$ at 20 wt% and 40 mesh is considered an optimal condition for enhancing PUFc.

CONCLUSIONS

1. Seashell waste was shown to be an efficient and sustainable bio-filler for polyurethane foam composites (PUFc). The X-ray fluorescence (XRF) analysis indicated that all examined seashell varieties were primarily composed of $CaCO_3$ (91 to 96 wt%), affirming their appropriateness as mineral fillers and supporting marine waste valorization.
2. The primary factors influencing the efficacy of PUFc were filler type, particle size, and filler loading, as these factors affected foam morphology. These parameters directly influenced the quality of dispersion and cell structure, thereby regulating the physical, mechanical, thermal, and moisture-related properties of the composites.
3. Particle size played a critical role in determining foam morphology and structural stability. Fine particles promoted uniform closed-cell structures by limiting cell growth, whereas coarse particles resulted in poor dispersion, structural heterogeneity, and weakened foam integrity.
4. At low to moderate filler loadings (10 to 20 wt%), constrained foam expansion and elevated solid percentage improved density and structural integrity. The peak density was consistently achieved at 20 wt% filler and 40-mesh particle size, signifying excellent dispersion.
5. Mechanical properties were optimized under these conditions as a result of stable cell morphology and improved stress transfer. Cockle shell exhibited the highest reinforcing efficiency, achieving a maximum tensile strength of 1580 kPa and a compressive strength of 1350 kPa at 20 wt% filler and 40 mesh. In contrast, excessive filler loading (30 wt%) caused filler agglomeration, void formation, and cell wall rupture, leading to mechanical degradation.

6. Thermal and moisture behaviors depended strongly on filler type and content. Although thermal conductivity increased moderately with filler additions, all values remained within acceptable insulation limits. An optimal balance of properties was achieved at 10 wt% filler and 80 mesh, where oyster shell-reinforced PUFc exhibited the lowest thermal conductivity and water absorption due to better preservation of a uniform closed-cell structure.
7. Cockle shell exhibited the highest mechanical properties, whereas oyster shell showed the best insulation performance, with the lowest thermal conductivity and water absorption. Green mussel shell displayed intermediate properties. These findings confirm that shell type, filler loading, and particle size influence the performance of PUFc and should be considered in the development of sustainable insulation materials.
8. The thermal conductivity, density, water absorption, and compressive strength values obtained in this study were generally within the ranges reported for bio-based insulation composites (Tesfie *et al.* 2024; Luo *et al.* 2026), indicating that seashell-reinforced PUFc has the potential to be a sustainable bio-based insulation material with performance comparable to previously reported bio-based insulation composites.

ACKNOWLEDGMENTS

Authors are grateful for the support of all research teams and the financial support provided by the Royal Thai Government Scholarship (Science and Technology), Grant No. 1-2023.

Conflict of Interest

Authors declare that they have no known competing financial interests or personal relationships that could have appeared to influence the work reported in this paper.

Use of Generative AI

QuillBot was used only for English grammar correction and language polishing. ChatGPT was used for language editing and improving the clarity of the manuscript. No AI tools were used for figures or tables.

REFERENCES CITED

Ahad, N. A., Lum, K. S., and Halim, K. (2023). "The effect of seashells as filler in epoxy composites," *Science Letters* 17(2), 119-129. https://doi.org/10.24191/sl.v17i2.22751

Akdogan, E., and Soykan, U. (2025). "Sustainable rigid polyurethane foam composites based on used palm oil and turkey feather fiber: structural, morphological, thermal, insulation and mechanical properties," *Clean Technologies and Environmental Policy* 27(9), 3969-3984. https://doi.org/10.1007/s10098-024-03080-x

Anwar, M. F., Yu, L. J., Lim, Y. M., Tarawneh, M. A., Se Yong, E. N., and Lai, N. Y. G. (2023). "Water absorption properties of polyurethane foam reinforced with paper pulp," *Materials Today: Proceedings*, in press (corrected proof). https://doi.org/10.1016/j.matpr.2022.12.156

Asfaw, N. T., Absi, R., B.A, L., and Ikram, E, A. (2024). "Assessment of the thermal and mechanical properties of bio-based composite materials for thermal insulation: A review," *Journal of Building Engineering* 97, article 110605. https://doi.org/10.3390/ma19061229

ASTM C518 (2017). "Standard test method for steady-state thermal transmission properties by means of the heat flow meter apparatus," ASTM International, West Conshohocken, PA, USA.

ASTM D570-98 (2018). "Standard test method for water absorption of plastics," ASTM International, West Conshohocken, PA, USA.

ASTM D1621-16 (2023). "Standard test method for compressive properties of rigid cellular plastics," ASTM International, West Conshohocken, PA, USA.

ASTM D2240-15 (2015). "Standard test method for rubber property durometer hardness," ASTM International, West Conshohocken, PA, USA.

ASTM D3574-17 (2017). "Standard test methods for flexible cellular materials slab, bonded, and molded urethane foams," ASTM Int., West Conshohocken, PA, USA.

Barszczewska-Rybarek, I., Jaszcz, K., Chladek, G., Grabowska, P., Okseniuk, A., Szpot, M., Zawadzka, M., Sokołowska, A., and Tarkiewicz, A. (2022). "Characterization of changes in structural, physicochemical and mechanical properties of rigid polyurethane building insulation after thermal aging in air and seawater," *Polymer Bulletin* 79(5), 3061-3083. https://doi.org/10.1007/s00289-021-03632-x

Basile, M. L., Triunfo, C., Gärtner, S., Fermani, S., Laurenzi, D., Maoloni, G., Mazzon, M., Marzadori, C., Adamiano, A., Iafisco, M., *et al.* (2024). "Stearate-coated biogenic calcium carbonate from waste seashells: A sustainable plastic filler," *ACS Omega* 9(10), 11232-11242. https://doi.org/10.1021/acsomega.3c06186

Bello, K. O., and Yan, N. (2024). "Mechanical and insulation performance of rigid polyurethane foam reinforced with lignin-containing nanocellulose fibrils," *Polymers* 16(15), article 2119. https://doi.org/10.3390/polym16152119

Choe, H., Lee, J. H., and Kim, J. H. (2020). "Polyurethane composite foams including $CaCO_3$ fillers for enhanced sound absorption and compression properties," *Composites Science and Technology* 194, article 108153. https://doi.org/10.1016/j.compscitech.2020.108153

Deraman, R., Nawi, M. N. M., Mydin, O. A. M., Ismail, H. M., Nordin, M. D. N., Sari, W. M., and Mohd-Danuri, M. S. (2022). "Production of roof board insulation using agricultural wastes towards sustainable building material," *Journal of Advanced Research in Fluid Mechanics and Thermal Sciences* 99(1), 66-89. https://doi.org/10.37934/arfmts.99.1.6689

Dukarska, D., Walkiewicz, J., Derkowski, A., and Mirski, R. (2022). "Properties of rigid polyurethane foam filled with sawdust from primary wood processing," *Materials* 15(15), article 5361. https://doi.org/10.3390/ma15155361

Ebereonwu, P., Dashak, D., and Ogah, C. (2022). "Investigation and characterization of flexible polyurethane foams from the use of chicken eggshells as fillers," (Preprint). https://doi.org/10.26434/chemrxiv-2022-mkc4d

Fidan, M. S., and Ertaş, M. (2020). "Bio-based rigid polyurethane foam prepared from apricot stone shell-based polyol for thermal insulation application – Part 2: Morphological, mechanical, and thermal properties," *BioResources* 15(3), 6080-6094. https://doi.org/10.15376/biores.15.3.6080-6094

Hadała, B., Zygmunt-Kowalska, B., Kuźnia, M., Szajding, A., and Telejko, T. (2024). "Thermal insulation properties of rigid polyurethane foam modified with fly ash – A

comparative study," *Thermochimica Acta* 731, article 179659. https://doi.org/10.1016/j.tca.2023.179659

Hernando Castro, S. M., Carabaño Rodríguez, R., López Arquillo, J. D., and Perea Álvarez De Eulate, M. (2025). "Comparative evaluation of construction insulation materials: Environmental performance across production, end-of-life, and beyond system boundaries," *Journal of Building Engineering* 99, article 111570. https://doi.org/10.1016/j.jobe.2024.111570

Kıstak, C., Yanen, C., and Aydoğmuş, E. (2025). "Advanced sustainable epoxy composites from biogenic fillers: Mechanical and thermal characterization of seashell-reinforced composites," *Applied Sciences* 15(15), article 8498. https://doi.org/10.3390/app15158498

Kuciel, S., Rusin-Żurek, K., and Kurańska, M. (2024). "The influence of filler particle size on the strength properties and mechanical energy dissipation capacity of biopoly(ethylene terephthalate) bioPET/eggshell biocomposites," *Recycling* 9(5), article 88. https://doi.org/10.3390/recycling9050088

Kustiyah, E., Roziafanto, A. N., Amrullah, M., Priadi, D., and Chalid, M. (2022). "Effect of calcium carbonate content on the mechanical and thermal properties of chitosan-coated poly(urethane) foams," *Indonesian Journal of Chemistry* 22(3), 827-834. https://doi.org/10.22146/ijc.72135

Li, T.-T., Xing, M., Wang, H., Huang, S.-Y., Fu, C., Lou, C.-W., and Lin, J.-H. (2019). "Nitrogen/phosphorus synergistic flame retardant-filled flexible polyurethane foams: Microstructure, compressive stress, sound absorption, and combustion resistance," *RSC Advances* 9(37), 21192-21201. https://doi.org/10.1039/C9RA02332A

Luo, S., Wang, S., Hu, C., Feng, L., Fan, H., and Ma, H. (2026). "Research on thermal insulation and durability of bio-based thermal insulation materials and its prospect of engineering application," *Materials* 19, article 1229. https://doi.org/10.1016/j.jobe.2024.110605

Olcay, H., and Kocak, E. D. (2022). "The mechanical, thermal and sound absorption properties of flexible polyurethane foam composites reinforced with artichoke stem waste fibers," *Journal of Industrial Textiles* 51(5_suppl), 8738S-8763S. https://doi.org/10.1177/1528083720934193

Pech-Can, G. E., Flores-Johnson, E. A., Carrillo, J. G., Bele, E., and Valadez-Gonzalez, A. (2024). "Mechanical properties of polyurethane foam reinforced with natural henequen fibre," *J. Compos. Sci.* 8(9), article 343. https://doi.org/10.3390/jcs8090343

Popovic, N.T., Lorencin, V., Strunjak-Perovic, I., and Coz-Rakovac, R. (2023). "Shell waste management and utilization: Mitigating organic pollution and enhancing sustainability," *Applied Sciences* 13, article 623. https://doi.org/10.3390/app13010623

Saadaoui, E., Ghazel, N., Ben Yahia, K., Tlili, N., Martín-Gómez, J. J., and Cervantes, E. (2017). "Genetic variation in Tunisian castor bean," *Botanical Sciences* 95(2), 271-281. https://doi.org/10.17129/botsci.850

Shao, H., Zhang, Q., Liu, H., Guo, W., Jiang, Y., Chen, L., He, L., Qi, J., Xiao, H., Chen, Y., *et al.* (2020). "Renewable natural resources reinforced polyurethane foam for use of lightweight thermal insulation," *Materials Research Express* 7(5), article 055302. https://doi.org/10.1088/2053-1591/ab8d87

Smithmaitrie, R., Jaafar, S., and Salaenoi, J. (2020). "Shell structure investigation and utilization of bio-extract fermented from green mussel shell," *Agriculture and Natural Resources* 2020, 415-422. https://doi.org/10.34044/j.anres.2020.54.4.10

Srichanachaichok, W., and Pissuwan, D. (2023). "Micro/nano structural investigation and characterization of mussel shell waste in thailand as a feasible bioresource of CaO," *Materials* 16(2), article 805. https://doi.org/10.3390/ma16020805

Suryawanshi, N., Jujjavarapu, S. E., and Ayothiraman, S. (2019). "Marine shell industrial wastes–an abundant source of chitin and its derivatives: Constituents, pretreatment, fermentation, and pleiotropic applications-a revisit," *Int. J. Environmental Science and Technology* 16(7), 3877-3898. https://doi.org/10.1007/s13762-018-02204-3

Wang, Z., Wang, C., Gao, Y., Li, Z., Shang, Y., and Li, H. (2023). "Porous thermal insulation polyurethane foam materials," *Polymers* 15(18), article 3818. https://doi.org/10.3390/polym15183818

Wieczorek, K., Bobak, Ł., and Bukowski, P. (2025). "From construction industry waste to high-performance insulation: Sustainable rigid polyurethane foams with recycled polyol," *Materials* 18(17), article 4179. https://doi.org/10.3390/ma18174179

Wiyono, P., Suprobo, P., and Kristijanto, H. (2016). "Characterization of physical and mechanical properties of rigid polyurethane foam," *ARPN Journal of Engineering and Applied Sciences* 11(24), 14398-14405

Article submitted: March 26, 2026; Peer review completed: May 31, 2026; Revised version received: June 21, 2026; Accepted: July 24, 2026; Published: September 30, 2026.
DOI: 10.15376/biores.21.4.11228-11246